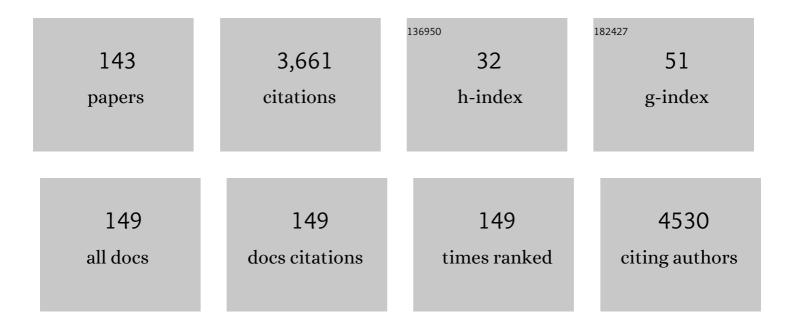
Dirk Mayer

List of Publications by Year in descending order

Source: https://exaly.com/author-pdf/7801710/publications.pdf Version: 2024-02-01



DIDK MAVED

#	Article	IF	CITATIONS
1	Highly selective and sensitive detection of glutamate by an electrochemical aptasensor. Analytical and Bioanalytical Chemistry, 2022, 414, 1609-1622.	3.7	13
2	Double-Resonant Nanostructured Gold Surface for Multiplexed Detection. ACS Applied Materials & Interfaces, 2022, 14, 6417-6427.	8.0	5
3	Gold nanostructures: synthesis, properties, and neurological applications. Chemical Society Reviews, 2022, 51, 2601-2680.	38.1	43
4	Single-Impact Electrochemistry in Paper-Based Microfluidics. ACS Sensors, 2022, 7, 884-892.	7.8	11
5	DNA aptamer selection for SARS-CoV-2 spike glycoprotein detection. Analytical Biochemistry, 2022, 645, 114633.	2.4	12
6	Delineating charge and capacitance transduction in system-integrated graphene-based BioFETs used as aptasensors for malaria detection. Biosensors and Bioelectronics, 2022, 208, 114219.	10.1	17
7	Inkjet printed Ta2O5 on a flexible substrate for capacitive pH sensing at high ionic strength. Sensors and Actuators B: Chemical, 2022, 369, 132250.	7.8	4
8	Prototype Digital Lateral Flow Sensor Using Impact Electrochemistry in a Competitive Binding Assay. ACS Sensors, 2022, 7, 1967-1976.	7.8	3
9	(Digital Presentation) Stochastic Impact Electrochemistry in a Lateral-Flow Sensor Architecture. ECS Meeting Abstracts, 2022, MA2022-01, 2116-2116.	0.0	0
10	Randomly positioned gold nanoparticles as fluorescence enhancers in apta-immunosensor for malaria test. Mikrochimica Acta, 2021, 188, 88.	5.0	18
11	PEDOT:PSSâ€Based Bioelectronic Devices for Recording and Modulation of Electrophysiological and Biochemical Cell Signals. Advanced Healthcare Materials, 2021, 10, e2100061.	7.6	92
12	Using Interdigitated Organic Electrochemical Transistors as Electrophysiological and Biochemical Sensors. Engineering Proceedings, 2021, 6, .	0.4	0
13	High Aspect Ratio and Light-Sensitive Micropillars Based on a Semiconducting Polymer Optically Regulate Neuronal Growth. ACS Applied Materials & Interfaces, 2021, 13, 23438-23451.	8.0	21
14	Inkjet-Printed and Electroplated 3D Electrodes for Recording Extracellular Signals in Cell Culture. Sensors, 2021, 21, 3981.	3.8	11
15	Engineering Electrostatic Repulsion of Metal Nanoparticles for Reduced Adsorption in Single-Impact Electrochemical Recordings. ACS Applied Nano Materials, 2021, 4, 8314-8320.	5.0	8
16	Multi-target electrochemical malaria aptasensor on flexible multielectrode arrays for detection in malaria parasite blood samples. Sensors and Actuators B: Chemical, 2021, 349, 130812.	7.8	17
17	SAW gas sensor based on extremely thin strain-engineered K0.7Na0.3NbO3 films. Applied Physics Letters, 2021, 119, .	3.3	4
18	An electrochemical aptamer-based biosensor targeting Plasmodium falciparum histidine-rich protein II for malaria diagnosis. Biosensors and Bioelectronics, 2021, 192, 113472.	10.1	16

#	Article	IF	CITATIONS
19	Polymer Nanopillars Induce Increased Paxillin Adhesion Assembly and Promote Axon Growth in Primary Cortical Neurons. Advanced Biology, 2021, 5, 2000248.	2.5	15
20	The Structure of the Electric Double Layer of the Protic Ionic Liquid [Dema][TfO] Analyzed by Atomic Force Spectroscopy. International Journal of Molecular Sciences, 2021, 22, 12653.	4.1	7
21	Origins of Leakage Currents on Electrolyte-Gated Graphene Field-Effect Transistors. ACS Applied Electronic Materials, 2021, 3, 5355-5364.	4.3	6
22	LSPR-based colorimetric immunosensor for rapid and sensitive 17β-estradiol detection in tap water. Sensors and Actuators B: Chemical, 2020, 308, 127699.	7.8	41
23	Surface Functionalization of Platinum Electrodes with APTES for Bioelectronic Applications. ACS Applied Bio Materials, 2020, 3, 7113-7121.	4.6	6
24	Electrochemical dual-aptamer biosensors based on nanostructured multielectrode arrays for the detection of neuronal biomarkers. Nanoscale, 2020, 12, 16501-16513.	5.6	31
25	Polyethylene glycol-mediated blocking and monolayer morphology of an electrochemical aptasensor for malaria biomarker detection in human serum. Bioelectrochemistry, 2020, 136, 107589.	4.6	29
26	Ultrasensitive antibody-aptamer plasmonic biosensor for malaria biomarker detection in whole blood. Nature Communications, 2020, 11, 6134.	12.8	85
27	Dualâ€Transducer Malaria Aptasensor Combining Electrochemical Impedance and Surface Plasmon Polariton Detection on Gold Nanohole Arrays. ChemElectroChem, 2020, 7, 4594-4600.	3.4	12
28	Label-Free Split Aptamer Sensor for Femtomolar Detection of Dopamine by Means of Flexible Organic Electrochemical Transistors. Materials, 2020, 13, 2577.	2.9	37
29	Surface Plasmon-Enhanced Switching Kinetics of Molecular Photochromic Films on Gold Nanohole Arrays. Nano Letters, 2020, 20, 5243-5250.	9.1	11
30	Tantalum(<scp>v</scp>) 1,3-propanediolate β-diketonate solution as a precursor to sol–gel derived, metal oxide thin films. RSC Advances, 2020, 10, 13737-13748.	3.6	3
31	Engineering Biocompatible Interfaces via Combinations of Oxide Films and Organic Self-Assembled Monolayers. ACS Applied Materials & Interfaces, 2020, 12, 17121-17129.	8.0	9
32	A Novel Ratiometric Electrochemical Biosensor Based on a Split Aptamer for the Detection of Dopamine with Logic Gate Operations. Physica Status Solidi (A) Applications and Materials Science, 2020, 217, 1900924.	1.8	18
33	A Highly Sensitive Amperometric Aptamer Biosensor for Adenosine Triphosphate Detection on a 64 Channel Gold Multielectrode Array. Physica Status Solidi (A) Applications and Materials Science, 2020, 217, 1900925.	1.8	9
34	Fully Printed μ-Needle Electrode Array from Conductive Polymer Ink for Bioelectronic Applications. ACS Applied Materials & Interfaces, 2019, 11, 32778-32786.	8.0	45
35	Amperometric Aptasensor for Amyloid-Î ² Oligomer Detection by Optimized Stem-Loop Structures with an Adjustable Detection Range. ACS Sensors, 2019, 4, 3042-3050.	7.8	44
36	Amplification of aptamer sensor signals by four orders of magnitude via interdigitated organic electrochemical transistors. Biosensors and Bioelectronics, 2019, 144, 111668.	10.1	37

#	Article	IF	CITATIONS
37	Tuning Channel Architecture of Interdigitated Organic Electrochemical Transistors for Recording the Action Potentials of Electrogenic Cells. Advanced Functional Materials, 2019, 29, 1902085.	14.9	42
38	Vapor-Phase Deposition and Electronic Characterization of 3-Aminopropyltriethoxysilane Self-Assembled Monolayers on Silicon Dioxide. Langmuir, 2019, 35, 8183-8190.	3.5	15
39	Monitoring amyloid-β proteins aggregation based on label-free aptasensor. Sensors and Actuators B: Chemical, 2019, 288, 535-542.	7.8	56
40	MEA Recordings and Cell–Substrate Investigations with Plasmonic and Transparent, Tunable Holey Gold. ACS Applied Materials & Interfaces, 2019, 11, 46451-46461.	8.0	13
41	Stability makes a difference. Nature Nanotechnology, 2019, 14, 925-926.	31.5	1
42	Neuronal adhesion and growth on nanopatterned EA5-POPC synthetic membranes. Nanoscale, 2018, 10, 5295-5301.	5.6	6
43	Electronic Responses to Humidity in Monolayer and Multilayer AuNP Stripes Fabricated by Convective Selfâ€Assembly. Physica Status Solidi (A) Applications and Materials Science, 2018, 215, 1700950.	1.8	5
44	Facile, non-destructive characterization of 2d photonic crystals using UV-vis-spectroscopy. Physical Chemistry Chemical Physics, 2018, 20, 4340-4346.	2.8	5
45	Asymmetric, nanoâ€ŧextured surfaces influence neuron viability and polarity. Journal of Biomedical Materials Research - Part A, 2018, 106, 1634-1645.	4.0	8
46	Shaping the Atomicâ€6cale Geometries of Electrodes to Control Optical and Electrical Performance of Molecular Devices. Small, 2018, 14, e1703815.	10.0	28
47	Aptamer-based electrochemical biosensor for highly sensitive and selective malaria detection with adjustable dynamic response range and reusability. Sensors and Actuators B: Chemical, 2018, 255, 235-243.	7.8	82
48	Shell-binary nanoparticle materials with variable electrical and electro-mechanical properties. Nanoscale, 2018, 10, 992-1003.	5.6	13
49	Molecular Orbital Gating Surface-Enhanced Raman Scattering. ACS Nano, 2018, 12, 11229-11235.	14.6	27
50	Engineering of Neuron Growth and Enhancing Cell-Chip Communication via Mixed SAMs. ACS Applied Materials & Interfaces, 2018, 10, 18507-18514.	8.0	16
51	Fabrication of patterned surface by soft lithographic technique for confinement of lipid bilayer. AIP Conference Proceedings, 2018, , .	0.4	1
52	Noise spectroscopy of tunable nanoconstrictions: molecule-free and molecule-modified. Nanotechnology, 2018, 29, 385704.	2.6	8
53	High Performance Flexible Organic Electrochemical Transistors for Monitoring Cardiac Action Potential. Advanced Healthcare Materials, 2018, 7, e1800304.	7.6	50
54	Nanoparticle stripe sensor for highly sensitive and selective detection of mercury ions. Biosensors and Bioelectronics, 2018, 117, 450-456.	10.1	15

#	Article	IF	CITATIONS
55	Flexible Microgap Electrodes by Direct Inkjet Printing for Biosensing Application. Advanced Biology, 2017, 1, 1600016.	3.0	21
56	The Influence of Supporting Ions on the Electrochemical Detection of Individual Silver Nanoparticles: Understanding the Shape and Frequency of Current Transients in Nanoâ€impacts. Chemistry - A European Journal, 2017, 23, 4638-4643.	3.3	33
57	Temperature-Dependent Electron Transport in Single Terphenyldithiol Molecules. Journal of Physical Chemistry A, 2017, 121, 2911-2917.	2.5	1
58	Flexible Gold Nanocone Array Surfaces as a Tool for Regulating Neuronal Behavior. Small, 2017, 13, 1700629.	10.0	19
59	Surface coupling strength of gold nanoparticles affects cytotoxicity towards neurons. Biomaterials Science, 2017, 5, 1051-1060.	5.4	7
60	Biosensing near the neutrality point of graphene. Science Advances, 2017, 3, e1701247.	10.3	68
61	Observation of chemically protected polydimethylsiloxane: towards crack-free PDMS. Soft Matter, 2017, 13, 6297-6303.	2.7	25
62	Controlled Engineering of Oxide Surfaces for Bioelectronics Applications Using Organic Mixed Monolayers. ACS Applied Materials & amp; Interfaces, 2017, 9, 29265-29272.	8.0	15
63	Electrochemical Nanocavity Devices. Springer Series on Chemical Sensors and Biosensors, 2017, , 199-214.	0.5	2
64	Ultraâ€ŧhin resin embedding method for scanning electron microscopy of individual cells on high and low aspect ratio 3D nanostructures. Journal of Microscopy, 2016, 263, 78-86.	1.8	38
65	Electrochemically triggered aptamer immobilization via click reaction for vascular endothelial growth factor detection. Engineering in Life Sciences, 2016, 16, 550-559.	3.6	19
66	Electrolyte-Gated Graphene Ambipolar Frequency Multipliers for Biochemical Sensing. Nano Letters, 2016, 16, 2295-2300.	9.1	36
67	3D Au–SiO ₂ nanohybrids as a potential scaffold coating material for neuroengineering. RSC Advances, 2016, 6, 47948-47952.	3.6	2
68	Single Molecule Characterization of UV-Activated Antibodies on Gold by Atomic Force Microscopy. Langmuir, 2016, 32, 8084-8091.	3.5	29
69	Simple and Flexible Model for Laser-Driven Antibody–Gold Surface Interactions: Functionalization and Sensing. ACS Applied Materials & Interfaces, 2016, 8, 21762-21769.	8.0	4
70	In Situ Analysis of the Growth and Dielectric Properties of Organic Self-Assembled Monolayers: A Way To Tailor Organic Layers for Electronic Applications. ACS Applied Materials & Interfaces, 2016, 8, 16451-16456.	8.0	10
71	Influence of Self-Assembled Alkanethiol Monolayers on Stochastic Amperometric On-Chip Detection of Silver Nanoparticles. Analytical Chemistry, 2016, 88, 3632-3637.	6.5	13
72	Multi‣evel Logic Gate Operation Based on Amplified Aptasensor Performance. Angewandte Chemie - International Edition, 2015, 54, 7693-7697.	13.8	85

#	Article	IF	CITATIONS
73	Tuning neuron adhesion and neurite guiding using functionalized AuNPs and backfill chemistry. RSC Advances, 2015, 5, 39252-39262.	3.6	18
74	Noise characterization of metal-single molecule contacts. Applied Physics Letters, 2015, 106, .	3.3	21
75	Immobilization and Surface Functionalization of Gold Nanoparticles Monitored via Streaming Current/Potential Measurements. Journal of Physical Chemistry B, 2015, 119, 5988-5994.	2.6	27
76	Gating capacitive field-effect sensors by the charge of nanoparticle/molecule hybrids. Nanoscale, 2015, 7, 1023-1031.	5.6	41
77	Electrochemical current rectification–a novel signal amplification strategy for highly sensitive and selective aptamer-based biosensor. Biosensors and Bioelectronics, 2015, 66, 62-68.	10.1	34
78	Nanocavity crossbar arrays for parallel electrochemical sensing on a chip. Beilstein Journal of Nanotechnology, 2014, 5, 1137-1143.	2.8	16
79	Electrochemical Oxidation as Vertical Structuring Tool for Ultrathin (<i>d</i> < 10 nm) Valve Meta Films. ECS Journal of Solid State Science and Technology, 2014, 3, P143-P148.	al 1.8	3
80	Onâ€chip fast scan cyclic voltammetry for selective detection of redox active neurotransmitters. Physica Status Solidi (A) Applications and Materials Science, 2014, 211, 1364-1371.	1.8	11
81	Electrochemical artifacts originating from nanoparticle contamination by Ag/AgCl quasi-reference electrodes. Lab on A Chip, 2014, 14, 602-607.	6.0	30
82	Advanced fabrication of Si nanowire FET structures by means of a parallel approach. Nanotechnology, 2014, 25, 275302.	2.6	13
83	Probing the effect of surface chemistry on the electrical properties of ultrathin gold nanowire sensors. Nanoscale, 2014, 6, 5146-5155.	5.6	27
84	Mechanically Controllable Break Junctions for Molecular Electronics. Advanced Materials, 2013, 25, 4845-4867.	21.0	192
85	Three-Terminal Single-Molecule Junctions Formed by Mechanically Controllable Break Junctions with Side Gating. Nano Letters, 2013, 13, 2809-2813.	9.1	103
86	Transport properties characterization of individual molecule device using noise spectroscopy: A new approach. AIP Conference Proceedings, 2013, , .	0.4	1
87	Generation of Protein Nanogradients by Microcontact Printing. Japanese Journal of Applied Physics, 2013, 52, 05DA19.	1.5	10
88	Origin of noise in structures with tuned nanoconstrictions. , 2013, , .		0
89	Functional peptides for capacitative detection of Ca ²⁺ ions. Physica Status Solidi (A) Applications and Materials Science, 2013, 210, 1030-1037.	1.8	1

90 Molecular Electronics: Mechanically Controllable Break Junctions for Molecular Electronics (Adv.) Tj ETQq0 0 0 rgBT/Overlock 10 Tf 50 6

#	Article	IF	CITATIONS
91	Transistor Functions Based on Electrochemical Rectification. Angewandte Chemie - International Edition, 2013, 52, 4029-4032.	13.8	18
92	A nanoporous alumina microelectrode array for functional cell–chip coupling. Nanotechnology, 2012, 23, 495303.	2.6	22
93	Noise and transport characterization of single molecular break junctions with individual molecule. Journal of Applied Physics, 2012, 112, .	2.5	29
94	Neuron Adhesion: Control of Cell Adhesion and Neurite Outgrowth by Patterned Gold Nanoparticles with Tunable Attractive or Repulsive Surface Properties (Small 21/2012). Small, 2012, 8, 3226-3226.	10.0	0
95	Field-effect Devices Functionalised with Gold-Nanoparticle/Macromolecule Hybrids: New Opportunities for a Label-Free Biosensing. Procedia Engineering, 2012, 47, 273-276.	1.2	1
96	Electrochemical current rectifier as a highly sensitive and selective cytosensor for cancer cell detection. Chemical Communications, 2012, 48, 2594.	4.1	26
97	Control of Cell Adhesion and Neurite Outgrowth by Patterned Gold Nanoparticles with Tunable Attractive or Repulsive Surface Properties. Small, 2012, 8, 3357-3367.	10.0	30
98	Determination of heavy metal ions by microchip capillary electrophoresis coupled with contactless conductivity detection. Electrophoresis, 2012, 33, 1247-1250.	2.4	20
99	Printing of Highly Integrated Crossbar Junctions. Advanced Functional Materials, 2012, 22, 1129-1135.	14.9	15
100	Direct electrochemistry of novel affinity-tag immobilized recombinant horse heart cytochrome c. Biosensors and Bioelectronics, 2012, 34, 171-177.	10.1	24
101	Cap size dependent transition from direct tunneling to field emission in single molecule junctions. Chemical Communications, 2011, 47, 4760.	4.1	34
102	A simple poly(dimethylsiloxane) electrophoresis microchip with an integrated contactless conductivity detector. Mikrochimica Acta, 2011, 172, 193-198.	5.0	14
103	Low impedance surface coatings via nanopillars and conductive polymers. Physica Status Solidi (A) Applications and Materials Science, 2011, 208, 1284-1289.	1.8	6
104	A simplified poly(dimethylsiloxane) capillary electrophoresis microchip integrated with a lowâ€noise contactless conductivity detector. Electrophoresis, 2011, 32, 699-704.	2.4	26
105	The Role of Oxidative Etching in the Synthesis of Ultrathin Single rystalline Au Nanowires. Chemistry - A European Journal, 2011, 17, 9503-9507.	3.3	22
106	Molecular Junctions Bridged by Metal Ion Complexes. Chemistry - A European Journal, 2011, 17, 13166-13169.	3.3	15
107	Patterned self-assembly of gold nanoparticles on chemical templates fabricated by soft UV nanoimprint lithography. Nanotechnology, 2011, 22, 295301.	2.6	32
108	Fabrication of nanogaps with modified morphology by potentialâ€controlled gold deposition. Physica Status Solidi - Rapid Research Letters, 2010, 4, 73-75.	2.4	11

#	Article	IF	CITATIONS
109	Rectified tunneling current response of bio-functionalized metal–bridge–metal junctions. Biosensors and Bioelectronics, 2010, 25, 1173-1178.	10.1	13
110	An Electrochemically Transduced XOR Logic Gate at the Molecular Level. Angewandte Chemie - International Edition, 2010, 49, 2595-2598.	13.8	53
111	Electrochemical current rectification at bio-functionalized electrodes. Bioelectrochemistry, 2010, 77, 89-93.	4.6	21
112	Molecular rectification in metal–bridge molecule–metal junctions. Physica Status Solidi (A) Applications and Materials Science, 2010, 207, 891-897.	1.8	6
113	Deformation of nanostructures on polymer molds during soft UV nanoimprint lithography. Nanotechnology, 2010, 21, 245307.	2.6	21
114	Molecular junctions based on intermolecular electrostatic coupling. Chemical Communications, 2010, 46, 8014.	4.1	17
115	Bidirectional immobilization of affinity-tagged cytochrome c on electrode surfaces. Chemical Communications, 2010, 46, 5295.	4.1	10
116	Noise spectroscopy of AlGaN/GaN HEMT structures with long channels. Journal of Statistical Mechanics: Theory and Experiment, 2009, 2009, P01046.	2.3	2
117	Electrochemical characterization of the effect of gold nanoparticles on the electron transfer of cytochrome c. Physica Status Solidi (A) Applications and Materials Science, 2009, 206, 489-500.	1.8	11
118	Impedimetric detection of covalently attached biomolecules on fieldâ€effect transistors. Physica Status Solidi (A) Applications and Materials Science, 2009, 206, 417-425.	1.8	18
119	UV nanoimprint lithography with rigid polymer molds. Microelectronic Engineering, 2009, 86, 661-664.	2.4	48
120	Resistively switching Pt/spin-on glass/Ag nanocells for non-volatile memories fabricated with UV nanoimprint lithography. Microelectronic Engineering, 2009, 86, 1060-1062.	2.4	26
121	Metal imaging on surface of micro- and nanoelectronic devices by laser ablation inductively coupled plasma mass spectrometry and possibility to measure at nanometer range. Journal of the American Society for Mass Spectrometry, 2009, 20, 883-890.	2.8	34
122	Determination of the Stability Constant of the Intermediate Complex during the Synthesis of Au Nanoparticles Using Aurous Halide. Journal of Physical Chemistry C, 2009, 113, 20143-20147.	3.1	13
123	Nanoimprint for future non-volatile memory and logic devices. Microelectronic Engineering, 2008, 85, 870-872.	2.4	24
124	Analyzing the electroactive surface of gold nanopillars by electrochemical methods for electrode miniaturization. Electrochimica Acta, 2008, 53, 6265-6272.	5.2	57
125	On Pattern Transfer in Replica Molding. Langmuir, 2008, 24, 6636-6639.	3.5	30
126	Micropatterned silicone elastomer substrates for high resolution analysis of cellular force patterns. Review of Scientific Instruments, 2007, 78, 034301.	1.3	80

Dirk Mayer

#	Article	IF	CITATIONS
127	Field-effect sensors with charged macromolecules: Characterisation by capacitance–voltage, constant-capacitance, impedance spectroscopy and atomic-force microscopy methods. Biosensors and Bioelectronics, 2007, 22, 2100-2107.	10.1	68
128	Electrochemical fabrication and characterization of nanocontacts and nm-sized gaps. Applied Physics A: Materials Science and Processing, 2007, 87, 569-575.	2.3	37
129	Fabrication of Large-Scale Patterned Gold-Nanopillar Arrays on a Silicon Substrate Using Imprinted Porous Alumina Templates. Small, 2006, 2, 1256-1260.	10.0	26
130	Surface activation of thin silicon oxides by wet cleaning and silanization. Thin Solid Films, 2006, 510, 175-180.	1.8	124
131	Interfacing Biology with Electronic Devices. Solid State Phenomena, 2005, 108-109, 789-796.	0.3	2
132	Scanning Probe Microscopic Studies of the Oriented Attachment and Membrane Reconstitution of CytochromecOxidase to a Gold Electrode. Langmuir, 2005, 21, 8580-8583.	3.5	18
133	Labelfree fully electronic nucleic acid detection system based on a field-effect transistor device. Biosensors and Bioelectronics, 2004, 19, 1723-1731.	10.1	245
134	SXPS and XANES Studies of Interface Reactions of Organic Molecules on Sulfide Semiconductors. , 2003, , 99-113.		0
135	In Situ Infrared Study of 4,4â€~-Bipyridine Adsorption on Thin Gold Films. Langmuir, 2002, 18, 4331-4341.	3.5	70
136	Distance tunnelling characteristics of solid/liquid interfaces: Au(111)/Cu2+/H2SO4. PhysChemComm, 2002, 5, 112.	0.8	5
137	Characterization of the mercaptobenzothiazole bonding on cadmiumsulfide by MO interpretation of N K XANES results. Chemical Physics, 2002, 277, 117-123.	1.9	6
138	Structural transitions in 4,4′-bipyridine adlayers on Au(111)—an electrochemical and in-situ STM-study. Journal of Electroanalytical Chemistry, 2002, 524-525, 20-35.	3.8	51
139	Angular-resolved XANES measurements of the polar and azimuthal orientation of alkanethiols on InP(110). Chemical Physics Letters, 1999, 311, 8-12.	2.6	12
140	XANES and XPS characterization of hard amorphous CSi x N y thin films grown by RF nitrogen plasma assisted pulsed laser deposition. Fresenius' Journal of Analytical Chemistry, 1999, 365, 244-248.	1.5	11
141	SXPS analysis of passivation and complexation on the CdS ($101\hat{A}^-0$) surface. Fresenius' Journal of Analytical Chemistry, 1998, 361, 689-692.	1.5	3
142	Characterization of organic adsorbates of CdS(100) surfaces by SXPS and XANES investigation. Journal of Electron Spectroscopy and Related Phenomena, 1998, 96, 245-251.	1.7	13
143	Nonequilibrium Fermi energy characteristics of n- and p-semiconductor electrodes under dark and photocurrents up to large band bending. Chemical Physics, 1996, 202, 39-51.	1.9	2